Comparative Study of Persistent Photoconductivity in GaP and GaN Nanostructures

Vitalie POSTOLACHE

National Center of Materials Study and Testing, Technical University of Moldova, Stefan cel Mare av. 168, Chisinau MD-2004, Republic of Moldova
postolache_vitalie@yahoo.com

***Abstract* — Relaxation of photoconductivity is investigated in bulk GaP and GaN substrates and epitaxial layers as compared to porous GaP samples and GaN nanomembranes. Porous GaP samples with different characteristic sizes of pores and walls are produced by electrochemical treatment in substrates with different carrier concentrations, while GaN nanomembranes are produced by means of surface charge lithography. It was found that different mechanisms are responsible for persistent photoconductivity in nanostructured GaP and GaN. The photoelectrical properties of bulk and nanoporous GaP are explained on the basis of randomly distributed potential barriers due to the high Te doping level and partial compensation in bulk samples and by a porosity controlled potential barriers pattern in porous samples. Metastable defects were found to be responsible for the persistent photoconductivity in both bulk GaN layers and nanomembrane. Enhancement of the optical quenching of persistent photoconductivity was observed in GaN nanomembranes. The possible nature of point defects responsible for these effects is discussed.**

***Index Terms* — Porous GaP, GaN nanomebrane, persistent photoconductivity, optical quenching.**

I. INTRODUCTION

Nanostructuring is known to significantly modify various properties of materials. Particularly, porosity induces a sharp increase in intensity of the near-band-edge photoluminescence in anodically etched GaP along with the emergence of blue and ultraviolet luminescence [1-3], strong enhancement of the non-linear optical properties [9,10], enhanced photoresponse in n-GaP electrodes [4,5], birefringence [6] and porosity-induced modification of the phonon spectrum [7,8], thus offering many potential advantages for device applications.

Nanostructuring is also expected to be a tool for modeling the photo-electrical properties of materials such as the long duration photoconductivity decay (LDPD), persistent photoconductivity (PPC), switching and memory effects [11-13]. It is known, that spatial barriers are responsible for these phenomena. Spatial barriers can be formed both by inhomogeneities of electrical properties and by nanostructured pattern of porous materials.

Metastable defects are another cause of PPC, which have been particularly speculated for wurtzite-type GaN epitaxial layers [14]. Different mechanisms were considered as origin of PPC in GaN, such as defects with bistable character [14,15], AX [16] or DX [17,18] centers. The identification of the origin of PPC in GaN epitaxial layers is especially important taking into account their great potential for applications in ultraviolet detectors [19,20] and field effect transistors (FET) [21,22]. The existence of metastable defects in GaN does not seem to have a negative impact on light emitters, while the PPC behavior associated with these defects can have a significant effect on the characteristics of FET and UV detectors based on AlGaN/GaN heterostructures, including sensitivity, noise properties, dark level, and response speed [21,23].

The goal of this study is to compare the photoelectrical properties of bulk single-crystalline and porous GaP from the one hand, and bulk GaN epitaxial layers and nanomembranes, on the other hand, in order to gain insight on the mechanism of PPC in these two materials. The influence of the porosity on the spatial distribution of the potential barriers in GaP, and the possible origin of metastable defects responsible for PPC in GaN are discussed.

II. SAMPLE PREPARATION AND EXPERIMENTAL DETAILS

(111)-oriented n-GaP substrates used in the present study were cut from Te-doped liquid encapsulation Czochralsky-grown ingots with the free electron concentrations $n_1 = 2 \times 10^{17}$ cm^{-3} and $n_2 = 1\times10^{18}$ cm^{-3} at 300 K. Porosity was introduced by anodic etching of samples for 30 min in a 0.5M aqueous solution of sulphuric acid at the current density 5mAcm^{-2} using a conventional electrochemical cell with a Pt working electrode. According to images obtained by a scanning electron microscope, the porous layers possess a honeycomb-like morphology with quasi-uniformly distributed pores, the average pore and skeleton thickness being about 150 and 50 nm for samples with initial carrier concentrations n_1 and n_2 respectively (let us denote them as porous samples GaP-1 and GaP-2).

Coplanar ohmic Ni-AuGe-Ni contacts were evaporated on samples subjected to subsequent rapid

thermal annealing. White light from a Narva halogen lamp passed through a MDR-2 monochromator as well as an Ar^+ laser beam was used for the photoconductivity (PC) excitation. Neutral density filters were used to reduce the intensity of the light at the sample. The samples were included in a circuit with a DC source and a electrometer for PC measurements. Since the PC decay time is long enough, a mechanical shutter was used in the PC relaxation experiments. The signal from the electrometer was introduced in an IBM computer via IEEE-488 interface for father data processing. The experiments were performed in a temperature interval 10 – 300 K, the samples being mounted in a LTS-22-C-330 Workhorse-type optical cryogenic system.

The wurtzite n-GaN layers were grown by lowpressure MOCVD on (0001) *c*-plane sapphire substrates. A buffer layer of 25 nm thick GaN was first grown at 510 °C. Subsequently a 3 μm thick n-GaN layer was grown at 1100 °C. The concentration of free electrons was of the order of 10^{17} cm^{-3}, while the density of threading dislocations was in the range of 10^9–10^{10} cm^{-2}.

A narrow self-supporting GaN membrane in the form of nanosheet was prepared by means of Surface Charge Lithography [24,25] through the following technological route. A rectangular area of GaN was treated by 30 keV Ga^+ ions at a dose as high as 10^{15} cm^{-2} to ensure the formation of a mesastructure under subsequent PEC etching. In addition to this, direct "writing" of the nanosheet was realized by FIB processing around the rectangular area, with the ion fluence being more than three orders of magnitude less than that used in the central area.

The sample morphology was studied using a VEGA TESCAN scanning electron microscope (SEM). A JEOL 7001F field emission SEM equipped with a Gatan XiCLone cathodoluminescence (CL) microanalysis system was used for comparative morphological and CL characterization. The monochromatic CL images were collected using a Peltier cooled Hamamatsu R943-02 photomultiplier tube. CL spectra were also collected with a PIXIS ccd camera with a 300 l/mm grating blazed at 500nm.

The radiation from xenon or mercury lamps passed through a monochromator as well as the 514 nm line of an Ar^+ laser were used for the excitation of photoconductivity in bulk GaN layers and nanomebranes. The samples were simultaneously or consequently irradiated by two beams of monochromatic radiation. One beam of radiation, called further "source A", provides either intrinsic or extrinsic excitation with photon energy $h\nu_A > 2.0$ eV. The second excitation source, called "source B", provides extrinsic excitation with photon energy $h\nu_B < h\nu_A$.

III. RESULTS AND DISCUTIONS

Figs. 2 - 6 compare the photoconductivity decay in bulk and porous GaP samples measured at temperatures of 150 K and 125 K at different excitation light intensities.

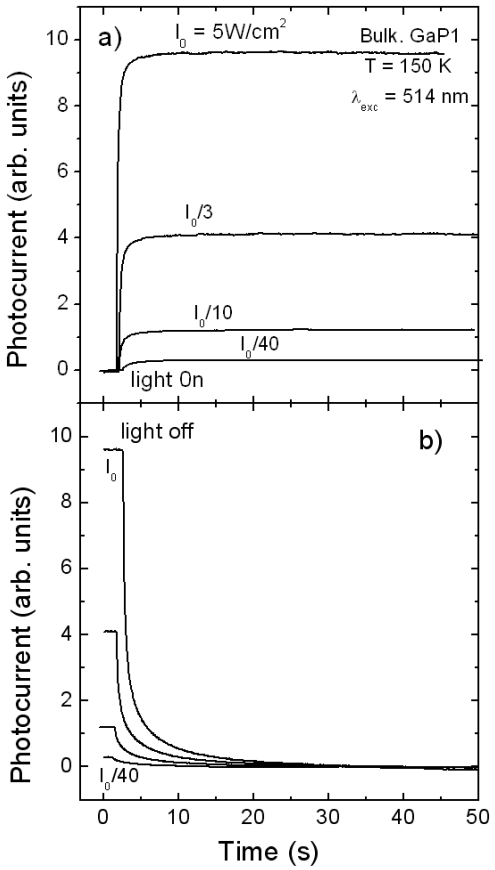

Fig. 1. PC transient in bulk GaP1 at different light intensities and T=150 K. a) light-on; b) light-off.

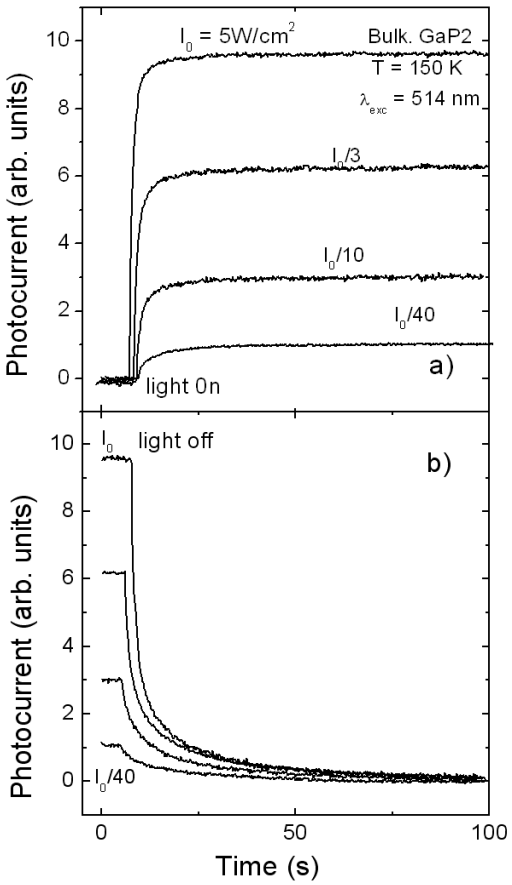

Fig. 2. PC transient in bulk GaP2 at different light intensities and T=150 K. a) light-on; b) light-off.

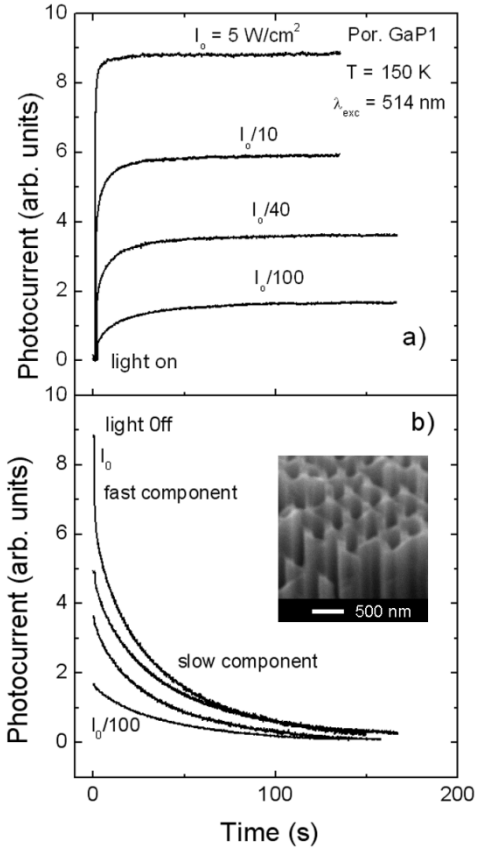

Fig. 3. PC transient in porous GaP1 at different light intensities and T=150 K. a) light-on; b) light-off. Inset is the SEM image of the sample.

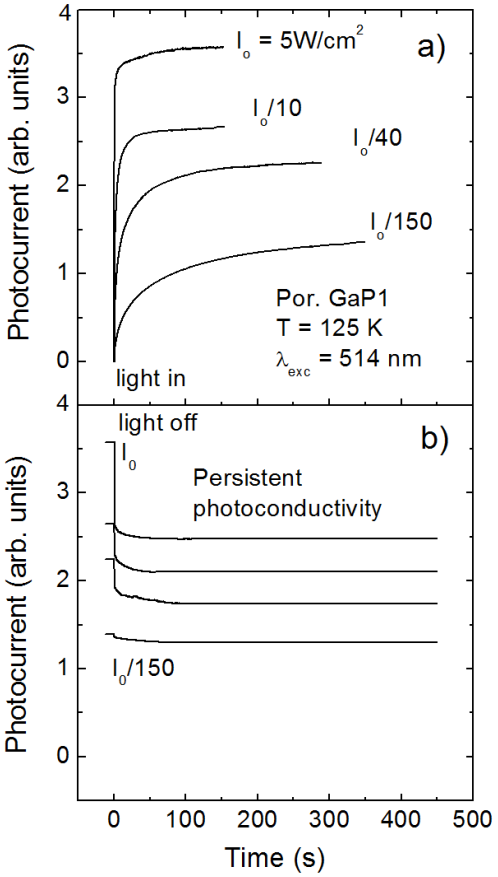

Fig. 5. PC transient in porous GaP1 at different light intensities and T=125 K. a) light-on; b) light-off.

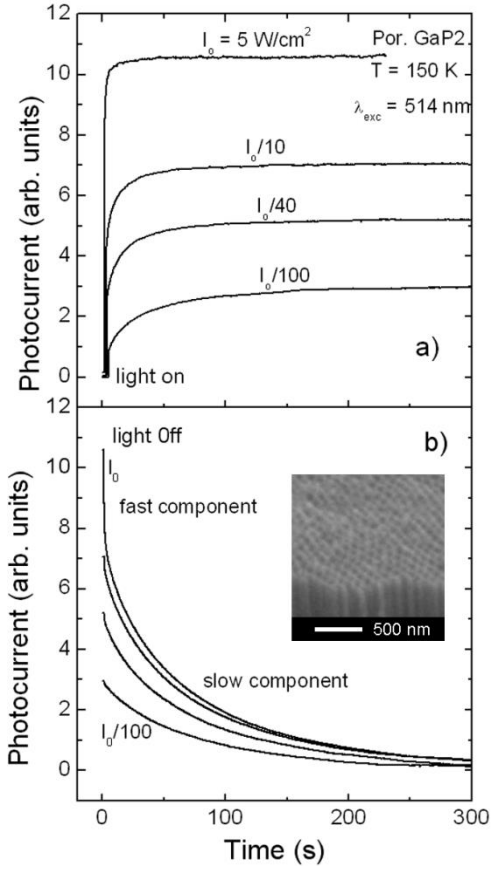

Fig. 4. The same as Fig. 3 but for porous GaP2 sample.

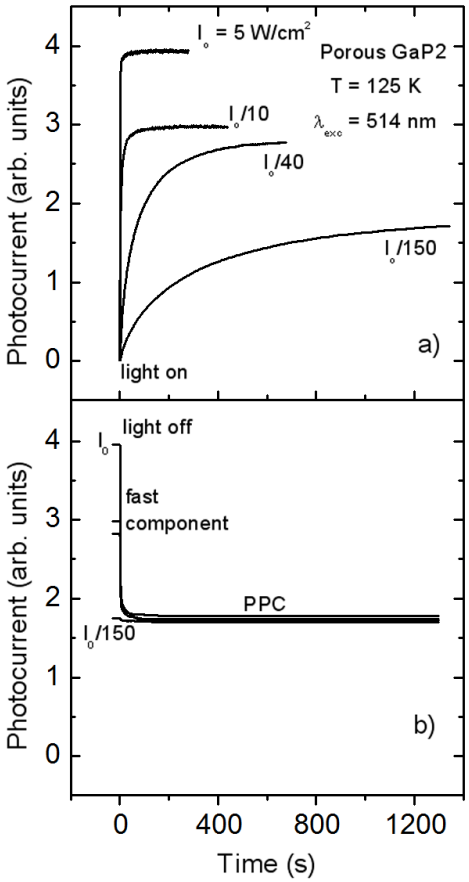

Fig. 6. The same as Fig. 5 but for porous GaP2 sample.

One can observe from figures 1 - 6 that in both bulk and porous samples the PC decay consists of two components: fast and slow, the last being more evident in porous sample.

The slow component manifests the characteristics inherent to LDPD: (i) LDPD is excited both by the intrinsic and extrinsic light; (ii) the PC relaxation is asymmetric in light on – light off; (iii) the transient time after the light turned on depends on the light intensity, it being decreased by the intensity increase, while the transient time after the light turned off is independent on the light intensity; (iv) the instantaneous transient time is temperature activated $\tau = \tau_0 \exp(E_b/kT)$, (the parameters τ_0 and E_b will be discussed further); (v) the value of E_b increases during the relaxation, therefore resulting in a transient slower than exponential. At low temperature τ can reach too high values, that the conductivity apparently doesn't change, i.e. the phenomenon of PPC is observed; (vi) the dependence of the slow component of the PC decay on the light intensity is sublinear, or it is linear at low intensities up to some I_c intensity and reaches saturation at higher light intensities. The value of I_c increases with increasing the temperature.

It is well known [11-13], that the LDPD and PPC phenomena are explained by the formation of spatial potential barriers due to the inhomogeneity of the samples. Actually in both bulk and porous GaP samples we observe the above mentioned phenomena, but they are more evident in porous samples and their nature is different in bulk and porous material.

The formation of randomly distributed potential barriers in bulk GaP is due to the high Te doping level and partial compensation. The amplitude of the potential relief in doped semiconductors is proportional to $(1\text{-}K)^{-1/3}$, where K is the compensation degree [11]. With lowering the temperature the compensation degree increases and the potential relief becomes more pronounced. One can see also from a comparison of Fig. 1 and Fig. 2 that the photoconductivity relaxation time is by a factor of three higher in the sample GaP2 as compared to GaP1. This difference is due to the increase of the compensation degree with increasing the free carrier concentration from $2*10^{17}$ cm^{-3} in sample GaP1 to $1*10^{18}$ cm^{-3} in sample GaP2.

In porous GaP the potential barriers are induced by porosity and they can be controlled by the morphology and porosity degree of the material.

The formation of spatial barriers in porous GaP was previously confirmed by thermally stimulated current and Raman spectroscopy [26]. The value of the local electrical fields in the porous sample produced from the substrate with carrier concentration of $1*10^{18}$ cm^{-3} deduced from these experiments is of the order of $E_0 \sim 5 \cdot x10^4$ V/cm [15]. Taking into account the ~50 nm dimensions of the pores in this sample one can calculate the value of $E_b \sim 250$ meV. LDPD and PPC are caused by the separation of the photo-excited carriers by these electric fields. Since in that case the carrier recombination is determined by the necessity to overcome the potential barrier E_b, the life-time of the excited carriers is described by the dependence $\tau = \tau_0 \exp(E_b/kT)$ and their stationary concentration is $\Delta n = \alpha\beta I\tau_0\{E_b(\Delta n)/kT\}$, where α and β are the absorption coefficient and quantum yeld, respectively; *I* stands for the light intensity, and τ_0 is the recombination time when the height of the potential barriers equals zero.

The value E_b derived from the temperature dependence of the mean value of the instantaneous time varies in the diapason 50 – 500 meV depending on the porosity degree. For instance, for the porous sample GaP1 it equals 110 meV (Fig. 7), while for the porous sample GaP2 in is around 210 meV (Fig. 8). The last value correlate well with the value of 250 meV estimated from Raman spectroscopy data. Raman spectroscopy also suggests a significantly lower value of the potential barrier for the GaP1 sample as compared to the GaP2 one.

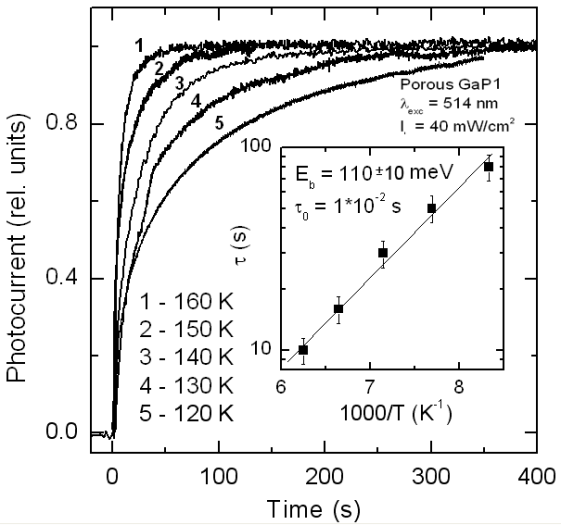

Fig. 7. Normalized PC decay in porous GaP1 at different temperatures. Inserted is the temperature dependence of the instantaneous time.

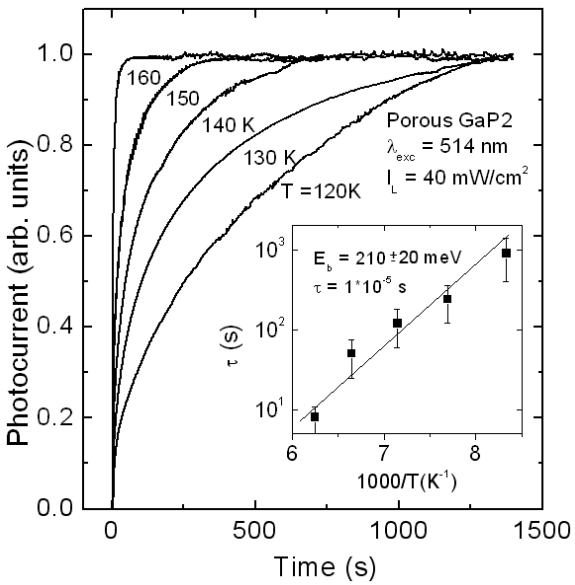

Fig. 8. The same as Fig. 7 but for porous GaP2 sample.

Evidently, the separation of the excited carriers creates electrical fields opposite to the existing potential barriers, therefore decreasing the amplitude of the potential relief. Then, the dependence $\Delta n(I)$ is sublinear except for the linear region at very low light intensities, where the value

of Δn is too low to change significantly the value of E_b. At high light intensities the Δn is saturated.

As one can see from Fig. 3 and Fig. 5, the slow component of the relaxation is far from saturation in the porous GaP1 sample at 150 K under the excitation of 125 mW (I_0/40), while it is close to saturation under these conditions of excitation at 125 K. With increasing the excitation intensity from 125 mW to 500 mW, the photocurrent increases by a factor of 1.2 only at the temperature of 125 K. The effect of saturation is even more pronounced in the GaP2 sample, so that the photocurrent is practically totally saturated at 125 K at the excitation power of 125 mW (Fig. 6).

Another is the mechanism of persistent photoconductivity in bulk GaN layers and nanomembranes, it being related to metastable defects, which were also suggested to be responsible for the yellow luminescence in GaN.

Figure 9 presents the cathodoluminescence spectra of a bulk GaN layer and a nanomembrane. One can see that the yellow luminescence band with the maximum at around 2.2 eV is much more intensive in the nanomembrane as compared to the bulk layer.

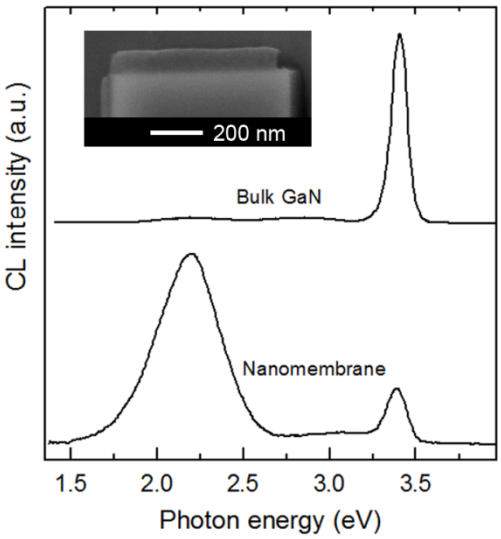

Fig. 9. CL spectra of a bulk GaN layer and a nanomembrane measured at 300 K. Inset is the SEM view of a narrow self-supporting GaN membrane.

The relationships between the yellow luminescence, the persistent photoconductivity (PPC), and the optical quenching (OQ) of photoconductivity have been previously investigated in GaN. Some authors suggested that PPC is related to yellow luminescence (YL) [14,27,28], while other found a relation between the yellow luminescence and OQ [29,30]. A detailed study of various GaN layers [31] by exciting the samples with two beams of monochromatic radiation of various wavelengths and intensities demonstrated that no correlation exists between PPC and yellow luminescence intensity, while a relation between PPC and OQ of photoconductivity was evidenced. These relations were described by a model stating that the PPC effect is associated with electron traps located at E_c – 2.0 eV, while OQ of PC arises from hole traps with the energy level near E_v + 1.0 eV. It was suggested that the deep defect involved in PPC is related to the nitrogen antisite, while gallium vacancy is responsible for OQ.

Figure 10 compares the effects of PPC and OQ in bulk GaN layers and nanomembranes. The persistent photoconductivity is induced by a radiation "source A" with wavelength of 365 nm, and the effect of the second excitation form the "source B" is investigated.

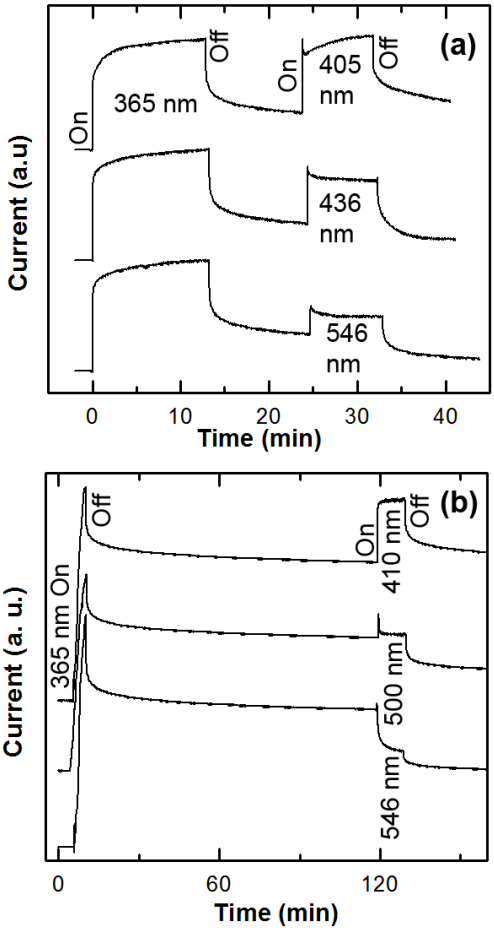

Fig. 10. a) The PC kinetics in a bulk GaN layer (a) and a nanomembrane (b) excited by a radiation source with wavelength of 365 nm followed by a second excitation with various wavelengths.

It is evident from Fig. 10 a, that the second excitation of bulk GaN layers with the radiation "B" induces PPC rather than OQ independently on the wavelength of radiation from the source B.

It was previously shown [31] that in bulk GaN layers OQ of photoconductivity occurs providing that the photon energies of the light sources satisfy the relations: (i) $h\nu_A$ > 2.0 eV; (ii) 1.0 eV < $h\nu_B$ < 2.6 eV; (iii) $h\nu_B$ < $h\nu_A$. Additionally, it was demonstrated that OQ of photoconductivity occurs only at low intensities of the source B radiation, if its quantum energy is from the interval 2.0 eV < $h\nu_B$ < 2.6 eV. On the other hand, the persistent photoconductivity is never quenched in bulk GaN layer.

Another behavior is observed in the GaN nano-membrane. As one can see from Fig. 10b, the radiation with the wavelength longer than 500 nm (the quantum energy $h\nu_B$ < 2.5 eV) produces OQ of the PPC induced by

the first source of radiation with the wavelength of 365 nm.

Therefore, one can suggest that the density of defects responsible for OQ of photoconductivity, including PPC, is significantly higher in GaN nanomembranes as compared to GaN layers. The metastable defects responsible for OQ in GaN were identified as gallium vacancies [31]. On the other hand, a strong YL was revealed in a surface layer of GaN nanowires as compared to weak YL in the bulk by studying the spatial distribution of defect-related and band-edge luminescence from GaN nanowires [32]. It was found that the surface YL layer completely quenches the band-edge luminescence as the nanowire width approaches a critical dimension. The surface YL was attributed to the diffusion and piling up of mobile gallium vacancies at the surface during growth. Taking this into account, one can suggest that the enhancement of YL in ultrathin suspended GaN membranes produced by surface charge lithography and the OQ of PPC are related to each other, and both these phenomena can be attributed to the same point defects which are more likely gallium vacancies.

IV. CONCLUSION

The results of this study demonstrate that the mechanisms responsible for persistent photoconductivity in nanostructured GaP and GaN are different. The persistent photoconductivity in bulk and nanoporous GaP is due to randomly distributed potential barriers which are related to the high Te doping level and partial compensation in bulk samples and to the nanostructured pattern in porous samples. The study of photoelectrical properties of bulk GaN layers and ultrathin membranes under excitation with two beams of monochromatic radiation of various wavelengths, where the first beam of radiation induces photoconductivity, while the second beam is used for the investigation of optical quenching effects, demonstrate the enhancement of optical quenching of photoconductivity in ultrathin GaN membranes as compared to bulk GaN layers. Taking into account the results of previous investigations and the results of this study, one can suggest that these two phenomena, i. e the enhancement of YL and the OQ of PPC in ultrathin membranes, are related to each other, and both these phenomena are due to the same point defects of gallium vacancies.

ACKNOWLEDGMENTS

This work was supported by the Academy of Sciences of Moldova under the grant No. 11.836.05.02A. The authors would like to thank his colleagues from the National Center for Materials Study and Testing for technical assistance and valuable comments.

REFERENCES

[1] A.I. Belogorohov, V.A. Karavanskii, A.N. Obraztsov, V.Yu. Timoshenco, *JETP Lett*., **60**, 274 (1994).

[2] A. Anedda, A. Serpi, V.A. Karavanskii, I.M. Tiginyanu, V.M. Ichizli, *Appl. Phys. Lett*., **67**, 3316 (1995).

[3] K. Kuriyama, K. Ushiyama, K. Ohbora, Y. Miyamoto, S. Takeda, *Phys. Rev. B*, **58**, 1103 (1998).

[4] I.M. Tiginyanu, I.V. Kravetsky, G. Marowsky, J.Monecke, H.L. Hartnagel, *Phys. Stat. Solidi (b)*, **221**, 557 (2000).

[5] I.M. Tiginyanu, I.V. Kravetsky, J. Monecke, W. Cordts, G. Marowsky, H.L. Hartnagel, Appl. Phys. Lett, **77**, 2415 (2000).

[6] B.H. Erne, D. Vanmaekelbergh, J.J. Kelly, *J. Electrochem. Soc*., **143**, 305 (1996).

[7] F. Iranzo Marin, M.A. Hamstra, D. Vanmaekelbergh, *J. Eletrochem. Soc*., **143**, 1137 (1996).

[8] E. Kukino, M. Amiotti, T. Takizawa, S. Arai, *Jap. J. Appl. Phys*, **34**, part 1, 177 (1995).

[9] I.M. Tiginyanu, G. Irmer, J. Monecke, H.L. Hartnagel, *Phys. Rev. B***, 55**, 6739 (1999).

[10] V.N. Denisova, B.N. Mavrina, V.A. Karavanskii, *Physics Lett. A*, **259**, 62 (1999).

[11] B.I. Shklovskii, A.L. Efros, *JETP*, **60**, 867 (1971); *JETP*, **61**, 816 (1971).

[12] M.K. Sheinkman, A.Ia. Shik, *FTP*, **10**, 209 (1976).

[13] Lowney Remiah R, Mayo Santos, *J. Electr. Matter.*, **21**, 731 (1992).

[14] C.V. Reddy, A. Balakrishnan, H. Okumura, and S. Yoshida, Appl. Phys. Lett. **73**, 244 (1998).

[15] C. Johnson, J.Y. Lin, H.X. Jiang, M.A. Khan, and C.J. Sun, Applo. Phys. Lett. **68**, 1808 (1996).

[16] J.Z. Li, J.Y. Lin, H.X. Jiang, A Salvador, A. Botchkarev, and H. Morkoc, Appl. Phys. Lett. **69**, 1474 (1996).

[17] J.Z. Li, J.Y. Lin, H.X. Jiang, M.A. Khan, and Q. Chen, J. Appl. Phys. **82**, 1227 (1997).

[18] J.Z. Li, J.Y. Lin, H.X. Jiang, M.A. Khan, and Q. Chen, J. Vac. Sci. Technol. **B15**, 1117 (1997).

[19] G.Y. Xu, A. Salvador, W. Kim, Z. Fan, C. Lu, H. Tang, et al, Appl. Phys. Lett. **71**, 2154 (1997).

[20] A. Osinsky, S. Gangopadhyay, R. Gaska, B. Williams, M.A. Khan, D. Kuksenkov, and H. Temkin, Appl. Phys. Lett. **71**, 2334 (1997).

[21] S.N. Mohammad, Z.-F. Fan, A. Salvador, O. Aktas, A.E. Botchkarev, W. Kim, and H. Morkoc, Appl. Phys. Lett. **69**, 1420 (1996).

[22] M.A. Khan, Q. Chen, C.J. Sun, J.W. Yang, M.S. Shur, and H. Park, Appl. Phys. Lett. **68**, 514 (1996).

[23] J.Z. Li, J.Y. Lin, H.X. Jiang, and M.A. Khan, Appl. Phys. Lett **72**, 2868 (1998).

[24] I. M. Tiginyanu, V. Popa, and O. Volciuc, Appl. Phys. Lett., **86**, 174102 (2005).

[25] I. Tiginyanu, V. Popa, and M. A. Stevens-Kalceff, Mater. Lett., **65**, 360 (2011).

[26] V. V. Ursaki, I.M. Tiginyanu, C. Ricci, A. Anedda, J. Phys.: Condens. Matter **13**, 4579 (2001).

[27] H.M. Chen, Y.F. Chen, M.C. Lee, and M.S. Feng, Phys. Rev. B **56**, 6942 (1997).

[28] H.M. Chen, Y.F. Chen, M.C. Lee, and M.S. Feng, J. Appl. Phys. **82**, 899 (1997).

[29] Z.C. Huang, D.B. Mott, P.K. Shu, R. Zhang, J.C. Chen, and D.K. Wickenden, J. Appl. Phys. **82**, 2707 (1997).

[30] T.Y. Lin, H.C. Yang, and Y.F. Chen, J. Appl. Phys. **87**, 3404 (2000).

[31] V.V. Ursaki and I.M. Tiginyanu, P.C. Ricci, A. Anedda, S. Hubbard, and D. Pavlidis, J. Appl. Phys. **94**, 3875 (2003).

[32] Q. Li, and G.T. Wang, Spatial Distribution of Defect Luminescence in GaN Nanowires, Nano Lett. **10**, 1554 (2010).